Article

Mechanical Properties of Spunlace Non-Wovens with a Porous Structure

Michał Sąsiadek , Anna D. Dobrzańska-Danikiewicz * , Maciej Niedziela , Waldemar Woźniak , Michał Szota

Posted Date: 18 October 2024

doi: 10.20944/preprints202410.1418.v1

Keywords: non-woven; porous structure; carding process; tensile strength; SEM

 doi:10.20944/preprints202410.1418.v1

Article

Mechanical Properties of Spunlace Non-Wovens with a Porous Structure

Michał Sąsiadek [1], Anna D. Dobrzańska-Danikiewicz [1,*], Maciej Niedziela [2], Waldemar Woźniak [3] and Michał Szota [4]

[1] Institute of Mechanical Engineering, University of Zielona Góra, 65-516 Zielona Góra, Poland
[2] Institute of Mathematics, University of Zielona Góra, 65-516 Zielona Góra, Poland
[3] Institute of Materials and Biomedical Engineering, University of Zielona Góra, 65-516 Zielona Góra, Poland
[4] Institute of Safety Engineering, Fire Academy, 01-629 Warsaw, Poland
* Correspondence: anna.dobrzanska.danikiewicz@gmail.com

Abstract: The paper describes the influence of the drum system construction of two modern carding machines on the porous structure of spunlace non-wovens composed of polyester and viscose. The non-woven fabric structure, including the number and size of the pores, determines the tensile strength of the composites obtained. The spunlace non-wovens were subjected to tensile strength tests in the machine, and cross directions and microscopic observations of their structure were made. The results of the experiments were used to determine the relationship between the strength of the material and the porosity of its structure. This knowledge was used to prepare recommendations for the manufacturer of wet wipes in order to enable the selection of a carding machine for the mass production of final products with strength properties that meet market requirements and satisfy the end customer.

Keywords: non-woven; porous structure; carding process; tensile strength; SEM

1. Introduction

A fresh perspective that has emerged in recent years suggests that improved materials will be crucial to the 21st century's process of fundamental transformation. Advanced materials clearly drive innovation because approx. 70% of all technical innovations can be directly or indirectly attributed to progress in the field of material engineering [1]. Therefore, their development will determine the future competitiveness of the European economy on the global market. Such a view was reflected in the Materials 2030 Manifesto, announced on 7 July 2022 [2]. Satisfying the growing demand for new materials and products requires a double-green and digital transformation. The success of the transformation is to be ensured through the application of advanced material solutions in combination with pro-ecological activities, including re-use, re-purposing, dismantling, recycling and refining, as well as modern digital technologies, such as tracking & tracing as well as digital twins [3–5]. In order to implement the assumptions of the Material Manifesto 2030, a pan-European Advanced Materials Initiative 2030 (AMI2030) was established [6]. The result of the work of AMI2030 is the Materials 2030 Roadmap [7], which juxtaposes advanced materials, including nanomaterials [8,9] and challenging, cross-cutting research and development technologies, with their significance for nine Materials Innovation Markets (MIMs). According to the concept adopted, the main opportunity to accelerate all aspects of material design and development is digitisation, and the key to success is to have reliable and easy access to the data. It is also necessary to increase the scalability of new materials, consisting of facilitating their spread to other sales markets and applications, through processes of optimisation, decarbonisation, mass customisation, zero defect production, improved multi-material manufacturing and new manufacturing technologies. Among the MIMs, apart from healthcare, construction, new energies, transport, home & personal care, packing, agriculture, and electronics, there are also textiles, to which the given article is devoted.

 doi:10.20944/preprints202410.1418.v1

Modern textiles are materials made of high-tech fibres and fabrics produced using advanced technology and machines [10]. Such a high-tech fibre is synthetic, functional and ecological [11]. The expectations of demanding product users mean that both natural fibres (e.g., cotton, wool, hemp) [12,13] and synthetic fibres (e.g., polyamide, viscose) [14] are not suitable for advanced applications. Functional fibres can have conductive [15] or antibacterial [16] properties. Avant-garde smart fibres allow for colour tuning [17], harvesting [18] and storing energy [19] and heat [20], and can also have shape memory [21]. Smart textiles sense and react to environmental conditions or external stimuli (e.g., mechanical, thermal, magnetic, chemical, electrical) through the presence of sensors, actuators or controlling units [22]. Smart textiles have applications in various sectors with promising expectations, such as cloth production, artificial intelligence, biotechnology, information, chaos theory and randomisations. For this reason, they are used in life clothing, medicine, health, ecology, environmental protection, military and aviation areas [23].

Non-wovens in ISO standard 9092 [24] and CEN EN 29092 [25] are defined as an engineered fibrous assembly, primarily planar, which has been given a designed level of structural integrity by physical and/or chemical means, excluding weaving, knitting or paper making. They key functions include as following [26]: absorbency, bacterial barrier, cushioning, filtering, flame retardancy, liquid repellence, resilience, softness, sterility, strength, stretch, and washability. The textile industry covers many areas related to processing textile raw materials. The last decade has brought an upward trend in the production of spunlace non-woven fabrics, which are ultimately soaked with surfactants in order to produce the final products used, such as washing and cleaning. The non-wovens are formed from mixtures of various fibres. These fibres, on an industrial scale, can be produced from natural polymers, synthetic polymers and inorganic materials. However, today, man-made materials completely dominate the production of non-wovens, accounting for as much as 99% of total production [27] and marginalising the importance of natural non-wovens. Polypropylene (PP) is most commonly used to produce non-wovens, ahead of polyester, regenerated cellulose, acrylic, polyamide, cotton and other speciality fibres [28].

The production of non-woven fabrics consists of the appropriate mixing of fibres and their bonding. Fibre bonding can take place, for example, in the water-needling process. The process that binds the fibres is carding, which is to form a continuous and homogeneous stream of fibre mixture called fleece to separate the bundles into individual fibres and agitate them intensively. Currently, the desired trend is to reduce the amount of raw material introduced while ensuring the required mechanical strength of the non-woven fabric. Manufacturers of carding machines are introducing new solutions in construction quite dynamically, primarily to increase the efficiency of the carding process and the quality of the non-wovens produced in terms of the homogeneity of fibre mixing and the strength of the non-wovens produced from them [28]. The constructions of modern carding machines are very complex and controlling them requires specialist knowledge and experienced operators who are responsible for selecting the most advantageous process parameters adapted to the processed raw material. It is important for the indirect recipient to provide him with a suitable non-woven fabric that meets the requirements for further processing [28–30].

In industrial settings, there are two main levels of quality control for fibre blending. The first level of quality control utilizes various image analysis tools and vision systems to detect inclusions (impurities) as well as the accumulation and thinning of fibres that occur during the non-woven fabrication process. The commonly used second level of quality control for fibre mixing occurs after the main non-woven fabric production process. Typical tests under industrial conditions are tests of the mechanical and physicochemical properties of non-woven samples, taken with the statistical precision indicated or according to the guidelines of the relevant industry's quality standards. However, the results of quality control at the two levels indicated cannot be used as a basis for inferring the correctness of the mixing of the fibres in terms of their meeting the expected strength properties, which is a source of further scientific investigation [31].

The state-of-the-art indicates that analyses of the carding process carried out in the last decade are mainly concerned with identifying and describing the basic processes that accompany the formation of the so-called fleece, composed of a mixture of different fibres. The most popular

 doi:10.20944/preprints202410.1418.v1

approach in the area is the classic take on the carding process, based on a single-cylinder model with a single fibre, collection and return system. A simple model of a single-drum carding machine, consisting of a main cylinder and a cooperating worker-stripper and doffer system, was described in [32], and the principles of working, stripping and interaction between card rollers were determined. By contrast Albrecht. W et al. [33] characterised the roller carding theory, giving the basic mathematical relationships for describing fibre flow in a model of a similar type of carding machine. Basic configurations of carding machines and different arrangements for randomising the web are presented in [33,34]. In a series of articles, Niedziela et al. [28–30] analysed the operation of two structurally different, double-drum carding machines. Papers [28] and [29] present a model of the carding process on a two-drum carding machine with one intermediate drum located between the main cylinders. Niedziela et al. [30] presented the results of the computer modelling of the operation of a two-drum carding machine in which, between the main cylinders, a system of four intermediate drums is located. For both kinds of carding machines, the dynamics of the fibre stream generation were examined, considering the uniformity of the created fleece's density. The mass balance of the fibres is considered when describing the carding dynamics. As part of the work, numerical simulations regarding the buildup of fibre flow over time, in connection to the fibre collecting coefficient and the number of worker-stripper systems, were also run and discussed. Moreover, the paper [30] developed a method for determining the fibre transfer coefficient, which enabled the derivation of relationships characterising the average lag time of fibres resulting from the circulation of fibres in the carding process.

The resulting carded non-woven fabrics were subjected to physicochemical and mechanical properties that are important for their further processing, such as weight, moisture content and strength. Santos. A. et al. [35] and Ivars. L. et al. [36], in the given aspect, studies of non-woven fabrics with added carbon fibres oriented towards determining their tensile and tear strength, taking into account the orientation and bond strength of the fibres, were conducted. Another aspect of non-woven testing was the study of the influence of the various setting parameters of the carding process on its final strength, as constituted by the water-needling process. In contrast, in the work by Roy et al. [37], an attempt was made to change the fibre orientation by varying the carding parameters, such as feeder speed, cylinder speed and receiver speed, while keeping the surface density of the fabrics the same. In addition, attention was devoted to the filtration process and the study of its influence on the needle process in the context of shaping the strength of the non-woven fabric. Finally, the optimum technological settings for the process analysed were developed, ensuring that non-woven properties would be acceptable to the end customer. Research into determining the relationship between the final strength of a non-woven fabric and the way it is manufactured is the subject of an article published by Hu.S. et al. [38]. It included an image analysis of the microstructure of the composite, composed of polyester and viscose fibres, to determine the effect of the carding process on the final strength of the material obtained after the drying process, i.e., the removal of excess water from the material.

Analysis of microscopic images of the non-woven fabric produced, mostly made using scanning electron microscopy (SEM), was used to assess the degree of the inter-correlation of its various parameters, such as pore size and orientation, machina and cross direction tensile strength, or the quality of the non-woven fabric, determined by the type of weaves and the number of inclusions, etc. For this purpose, it is possible to use artificial neural networks, as proposed by Hou.J. et al. in the work [39], to effectively reconstruct the spatial structure of the fabricated non-woven fabric. A similar issue is also addressed in article [40], in which Chen.Y. et al. propose to process microscopic images of high and low frequency in their multi-focus fusion process in order to determine the diameter of the fibres, as well as the orientation and porosity of the non-woven fabric. Similar problems were also raised in the manuscript developed by Kim.D. [41]. Analysis of microscopic images of non-wovens can also be used to determine deformation and changes in fibre orientation. Stolyarov.O. and Ershov.S. [42] determined the mechanical properties of the non-woven structure at three successive stages of deformation. In addition, the relationships between the change in fibre orientation, the angle of orientation, and the degree of material deformation were determined.

 doi:10.20944/preprints202410.1418.v1

In light of the selected research areas outlined above, the article responds to the market's reported expectations of absorbent wipes manufacturers based on non-woven polyester and viscose fabrics. The global wet wipes market is very broad and includes the following applications [27]: personal care and hygiene, household care, medical and healthcare aa well as industrial ones. The research results can, therefore, directly transfer to applications in industrial enterprises, which, while fighting for a competitive position in a mutable sector, are vitally interested in improving production efficiency while maintaining a high quality of the final product. It is important to note that the porous structure of non-wovens is influenced by the structural design of the carding drum systems, which was proven as a result of a comparative analysis of two alternative modern carding machines. The structure of the resulting non-woven fabric, including the number, size and orientation of the pores in relation to the non-woven flow direction during the manufacturing process, determines the machine and cross-direction tensile strength of the composite material obtained as a result of carding. It is evidenced by the results of the experiments performed, including tensile strength tests presented in the paper. The mechanical test results obtained and the SEM observations, along with image analysis made were used to determine the relationship between the strength of the material and the porosity of its structure. The information can directly transfer into specific technical solutions used in enterprises producing wet wipes for consumer applications, such as personal and household care, and professional applications in industry or medical areas.

2. Materials and Methodology

2.1. Materials

The input material used in the production process of non-woven fabric is a mixture of polyester and viscose fibres in proportions of 80% and 20%, respectively. These materials are commercially available on the market and are used on a large scale in the textile industry.

The basic parameters that are used to determine the properties of fibres are as following: linear density, breaking tenacity, breaking elongation and cut length. The measure of the fibre linear density is decitex, abbreviated as [dtex], which means the weight in grams of 10,000 metres of yarn. The second textile-specific measure is the fibre breaking tenacity, which is expressed in grams per decitex [g/dtex]. Table 1 presents the basic parameters of the fibres which are the input material for the production of non-wovens analysed in this paper.

Table 1. Parameters of fibres from which the non-woven fabric was fabricated.

Fibre Parameter	Polyester	Viscose
Linear density [dtex]	1.6	1.7
Breaking tenacity [g/dtex]	6.6	2.2
Breaking elongation [%]	25.0	19.5
Cut length [mm]	38	40

2.2. Production Tests on Non-Woven Fabrics

Two production tests carried out on a real production line were performed to determine the interdependencies between the carding process parameters of the fibre mixture and the strength properties of the final non-woven fabric. Two different carding machines in a sequential arrangement (Figures 1 and 2) were installed in the analysed prototype technological line. The arrangement of the intermediate drums between the two main cylinders is the main point of difference between the carding machine No. 1 and the carding machine No. 2.

Feeding the fibre deck to the R_0 feed roller and take-in roller of the carding machine No. 1 (Figure 1) starts the carding process. These rollers, together with the cleaning rollers, then transfer all the fibres to the main cylinder, i.e., the T_1 tambour. Five pairs of carding rollers in the R_w worker roller—the R_s stripper roller system are designed on the circumference of the T_1 cylinder. Carding rollers are used to crush and mix the twisted and joined fibres called tufts. The next stage of the process is the transport of the fleece using the two parallel subassemblies, i.e., shafts R_1 and R_2, as well as R_3 and R_4

 doi:10.20944/preprints202410.1418.v1

to the T_2 master cylinder. The T_2 cylinder is also equipped with a set of five pairs of worker-stripper rollers, which are used for further finer shredding and mixing of fibres. The structural construction of the T_2 tambour and the associated carding roller arrangements is the same as for the T_1 tambour. The next carding stage is to pull the fibre from the T_2 tambour by the D_1 doffer roller. Finally, the fibre in the form of a homogeneous web is transported to the conveyor by the R_5 condenser and the R_6 take-off roller. The green lines in Figure 1 indicate the fibres flow in individual carding assemblies, starting from the entrance (left side—the R_0 drum) to the exit (right side—the R_6 drum). The structural construction of the carding machine No. 1 is a system of four fibre transfer drums located between the main cylinders. The solution allows the processing of fibre material in the range of 25 to 100 g/m^2, as indicated in the technical documentation.

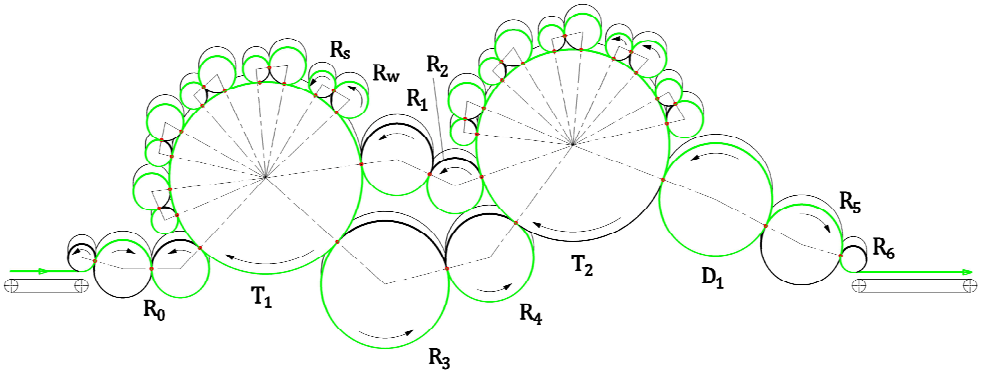

Figure 1. Schematic image of carding machine No. 1.

In carding machine No. 2 (Figure 2), the fibres between the main cylinders are transferred using only one drum, resulting in a slightly narrower fibre production range of 25 to 80 g/m^2, as per the technical documentation. The construction of this carding machine No. 2 differs from carding machine No. 1, primarily in placing intermediate drum transporting fibres between the main cylinders, marked as T_1 and T_2. The arrangement consists of using the R_1 intermediate cylinder. In addition, as in the case of carding machine No. 1, in carding machine No. 2, there are 5 worker-stripper assemblies on each main cylinder. The fibre mixture (fleece) is transported analogously as in the case of carding machine No. 1. The green lines Figure 2 indicate the fibres flow in individual carding assemblies, starting from the entrance (left side—the R_0 feed roller) to the exit (right side—the R_3 take-off roller).

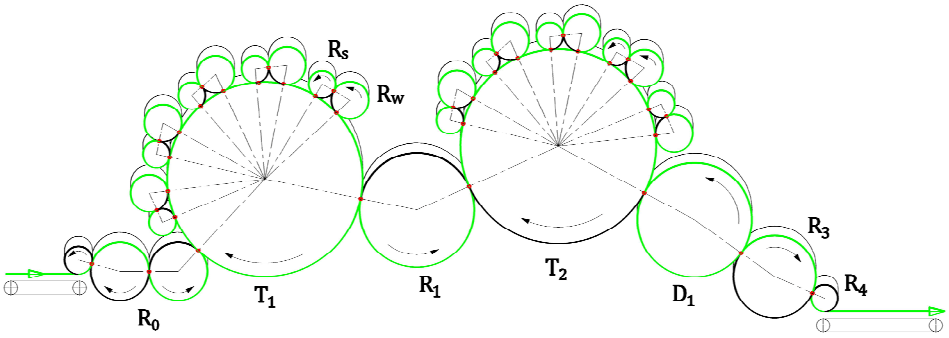

Figure 2. Schematic image of carding machine No. 2.

Differences in the structural construction of carding machines affect the operation speed of individual structural elements, i.e., main cylinders, worker-stripper assemblies and other working drums of carding machines. It results in a significant increase in process efficiency of carding machine No. 1 compared to a single-drum carding machine.

 doi:10.20944/preprints202410.1418.v1

Two tests were planned and carried out on an actual production line to produce a 40 g/m^2 non-woven fabric consisting of 80% polyester and the remaining 20% viscose, with the speed of process 190 m/min. The following operating configurations of carding machines were used:

- Test 1—production of non-woven fabric using carding machine No. 1;
- Test 2—production of non-woven fabric using carding machine No. 2.

2.3. Image Digital Analysis of the Non-Woven Fabric Structure

Microscopic examinations were performed on pre-sampled non-woven fabric samples using a JEOL JSM 7600F scanning electron microscope. The digital image of the surface of the spunlace non-woven fabric produced by carding machine No. 1 and carding machine No. 2 was automatically evaluated and analysed. For this purpose, an algorithm was developed to process and evaluate the image based on the images taken. The created algorithm was first used to measure the number of pores, estimate their size, and determine their shape and orientation. Then, the influence of these parameters on the mechanical properties of the non-woven fabric was determined, considering the type of carding machine used for its production.

The intensity function values that determine the grey level are used to describe the digital image as a two-dimensional table. A pixel is the smallest element of a digital image. For each sample of non-woven fabric used in the study, produced by the process described in Section 2.2, digital images were taken using a microscope. Each digital image is 1280 × 870 pixels, corresponding to 3668 × 2490 μm expressed in length units. Digital SEM image showing the non-woven fabric produced by carding machine No. 1 is shown in Figure 3a, and the non-woven fabric produced by carding machine No. 2 in Figure 3b.

Image modelling was performed in several stages, forming part of the execution algorithm. First, the grayscale image is converted to a binary image using Otsu Method [43] thresholding, followed by removing imperfections and texture distortions by applying morphological operations. The resulting monochrome image contains black pixels with a value of 0 corresponding to the fibres and white pixels with a value of 1, representing the pores, i.e., voids between the fibres. Figure 4a shows monochrome images created by converting a digital SEM image of a non-woven fabric produced on carding machine No. 1. An analogous monochrome image of a non-woven fabric produced using carding machine No. 2 is shown in Figure 4b.

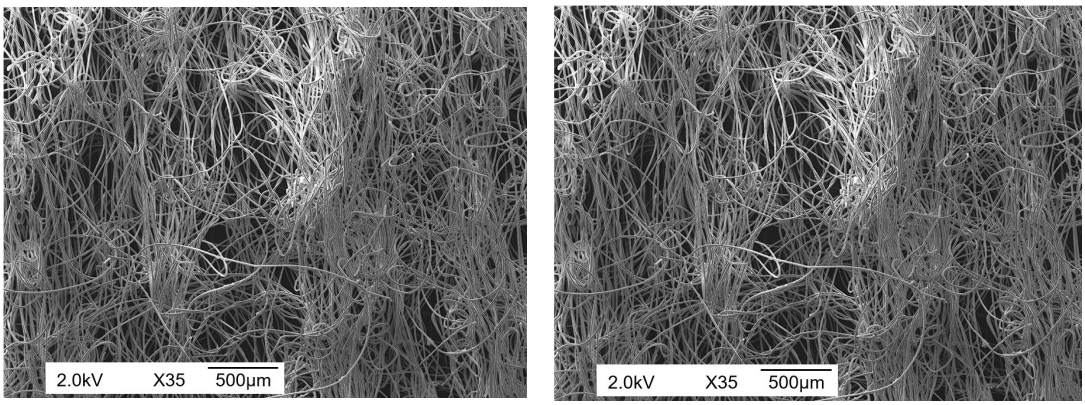

(**a**) (**b**)

Figure 3. Digital SEM image of the spunlace non-woven surface: (**a**) produced by carding machine No. 1; (**b**) produced by carding machine No. 2.

 doi:10.20944/preprints202410.1418.v1

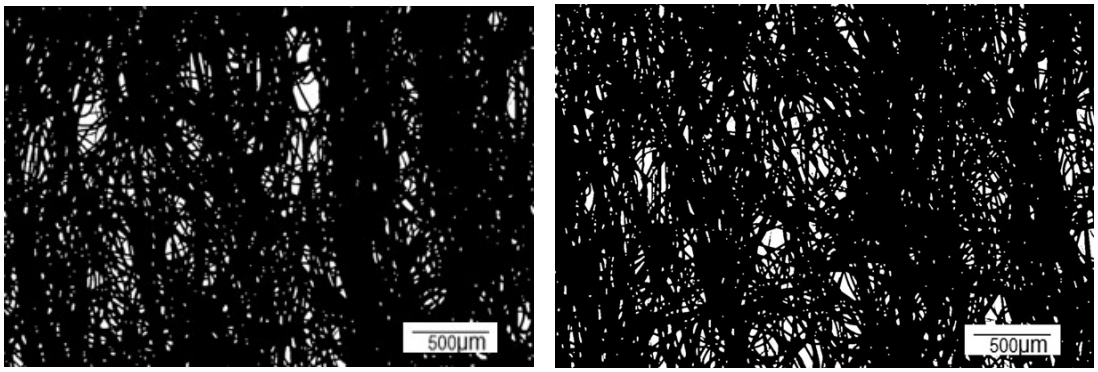

(**a**) (**b**)

Figure 4. Image modelling: monochrome image of a non-woven fabric: (**a**) produced by carding machine No. 1; (**b**) produced by carding machine No. 2.

In the next step of the algorithm, areas representing pores occurring between fibres were delineated. A function was used to determine the contours of all areas of uniformly coherent pixels in white with values of 0. At the same time, each contour defines a polygon, which defines the area of occurrence of a given pore bounded by a closed broken line. Geometric determination of pores using polygons allows to determine their surface areas, which are designated by the symbol *P*. The main emphasis of the research process was to analyse the relationship between the key parameters specifying the pores and the strength of the non-woven fabric. The analysis was therefore limited to only larger areas that can have a real impact on the tensile strength of the non-woven fabric, as measured in tests performed in the machine direction (MD) and cross direction (CD). Only those pores with an area greater than 1000 µm² qualified for further analysis. It brought the average number of pores selected to 180 for each SEM image subjected to digital image analysis. This represented approximately 10 per cent of all detected mono-contiguous areas with pixel values of 0.

Determining the parameters characterising the shape of the selected pores is the next step in the procedure according to the created algorithm. In this step, an ellipse with a 95% confidence interval is fitted to the set of pixels. It allows data on the position of a set of monochrome white pixels to be obtained. It is also possible to determine the dimensions of the ellipse by measuring its major and minor axes. Thus, the location of a given area, as well as its size and shape, are known. On this basis, the shape of a given area was estimated (Figure 5). Mathematically, the measure of circularity is defined by eccentricity *e*, whose value is expressed by Formula (1), which is used in geodetic and cartographic calculations [44].

$$e = \sqrt{1 - \left(\frac{b}{a}\right)^2}, \tag{1}$$

where:

a—half of the ellipse major axis;

b—half of the ellipse minor axis.

The eccentricity value is between 0 and 1. Eccentricity takes the value 0 if and only if $a = b$. In this particular case, the ellipse is a circle. Striving for the value of the eccentricity to 1 is the elongation of the ellipse. In this case, the ratio of half of the ellipse major axis and half of the ellipse minor axis $\frac{a}{b}$ tends to infinity.

Another parameter for determining the shape of the non-woven pores is the flattening of ellipse *f*. The parameter is used in geodetic and astronomical computations and determining the degree of deviation of the ellipse from a spherical shape, which is expressed by Formula (2) [45],

$$f = 1 - \frac{b}{a} \tag{2}$$

If the parameter *f* is close to zero, it means that $a \approx b$ and the shape of the analysed pore are close to a circle. The more the ellipse is extended, i.e., the greater the difference between the ellipse major and minor axes, the more the *f* factor approaches 1.

 doi:10.20944/preprints202410.1418.v1

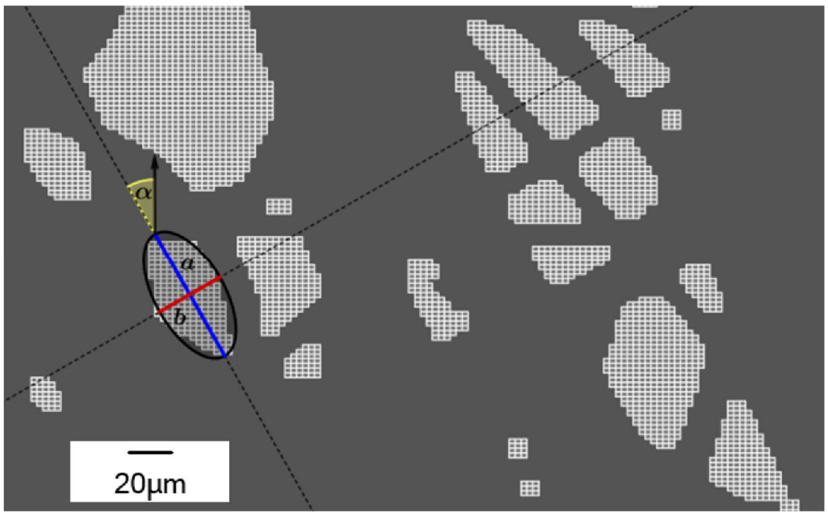

Figure 5. Image modelling: ellipse fitted to a set of pixels (white) with a 95% confidence interval (black). Callouts: blue—the *a* ellipse major axis; red—the *b* ellipse minor axis; pale yellow—the α angle of inclination of the ellipse relative to the axis of fibre flow direction in the production process.

In the last step of the procedure, according to the algorithm developed, the parameter determining the location of the study area (pore) was determined. The angle of inclination of the α ellipse major axis, relative to the axis of fibre flow direction in the production process, i.e., machine direction (MD), expressed in degrees [°], is indicated in Figure 5 in the pale yellow with a black narrow. Formally, if the ellipse is inclined to the right, the slope is positive, while when the ellipse is inclined to the left, the slope is negative. The direction of ellipse inclination in relation to the fibre flow direction in the manufacturing process does not affect the tensile strength of the non-woven fabric in the machine or cross directions. Therefore, its absolute value $|\alpha|$ for the calculations was adopted. In addition, ellipses were divided into groups with respect to the $|\alpha|$ values obtained. A division of the ellipses into 3 groups with respect to their inclination to the vertical axis, defining the direction of the carding machine, was adopted. If $0 \leq |\alpha| < 30°$, then the orientation is vertical. If $30° \leq |\alpha| < 60°$, then the orientation is oblique. If $60° \leq |\alpha| \leq 90°$, then the orientation is horizontal.

2.4. Tensile Strength Research

The non-wovens produced in the production tests described (Section 2.2) were subjected to machine and cross direction tensile strength tests in accordance with the current ISO 9073-3:2023 standard [46]. The tests were carried out using a testing machine, such as Zwick Z050, on technological specimens measuring 100 × 100 mm. A set of five (5) such specimens cut at 100-metre intervals were prepared sequentially from the manufactured non-woven fabric in Tests 1 and 2. Each set contained seven samples evenly spaced with respect to the width of the production line. All samples taken were tested in the machine direction (MD), i.e., in line with the direction of production and cross to it (CD) to determine their tensile strength.

3. Results

3.1. Pore Analysis

The actual testing process was carried out on a new spunlace non-woven fabric production line consisting of two different carding machines, described in Section 2.2 of this paper. The manufactured spunlace non-woven fabric was subjected to a tensile strength test. The strength test was carried out on 5 samples each, produced using carding machine No. 1 and carding machine No. 2, respectively. After that, 15 digital images were taken for each sample tested. The locations for the digital images were precisely selected and placed in the points of a homogeneous grid corresponding to a 50 × 100 mm sample. A total of 150 images were used to carry out the simulation using the algorithm

 doi:10.20944/preprints202410.1418.v1

described in Section 2.3, of which 75 showed the non-woven fabric produced on carding machine No. 1. Another 75—the non-woven fabric produced on carding machine No. 2. Observation of the digital images made it possible to measure the *P* pore surface area and the *N* pore number. The results of the measurements and the *e*, *f* and $|\alpha|$ estimated parameters determining the shape and orientation of the pores were grouped and averaged. Preliminary microscopic observations of the nonwoven fabric showed that the $|\alpha|$ absolute value affects the MD and CD tensile strength of the tested non-woven fabric. Horizontal orientation has a greater impact on MD tensile strength than CD, while the opposite behaviour is observed for vertical orientation. In addition, the pore size also affects the results of the MD and CD tensile test. For the analysis of the effect of pores on the tensile strength of non-woven fabrics, the algorithm input data was divided into groups according to two criteria. The first classification criterion is the *P* pore surface area (Table 2). The second classification criterion is the $|\alpha|$ absolute value of the pore inclination angle to the non-woven flow direction during manufacturing (Table 3).

The results obtained were then averaged for each of the detailed groups mentioned, based on a total of 75 microscopic images comprising five samples for each carding machine. The number of all areas analysed and their total area are shown in Table 4. The mean and total surface area and pore counts for groups A, B and C are shown in Table 5. The averaged results of area *P*, orientation, eccentricity *e* and flattened ellipse *f* for groups a, b and c are included in Table 6.

Table 2. Groups of pores classified by surface area.

Group Designation	Pore Surface Area [µm²]	Type of Area
A	$P \geq 5000$	large area
B	$2000 \leq P < 5000$	medium area
C	$1000 \leq P < 2000$	small area

Table 3. Groups of pores classified according to pore angle.

Group Designation	Pore Angle [°]	Orientation Type
a	$0 \leq \|\alpha\| < 30$	vertical orientation
b	$30 \leq \|\alpha\| < 60$	oblique orientation
c	$60 \leq \|\alpha\| < 90$	horizontal orientation

Table 4. Number of pores and total surface area of the areas detected for Tests 1 and 2.

Test 1		Test 2	
Number of Pores	Pore Surface Area $[mm^2]$	Number of Pores	Pore Surface Area $[mm^2]$
13,467	28.64	13,847	29.86

Table 5. Number of pores, percentage share, average and total pore surface area for groups A, B and C.

Variable	Test 1			Test 2		
	Group A	Group B	Group C	Group A	Group B	Group C
Number of pores [u]	649.00	3993.00	8825.00	706.00	4037.00	9104.00
Share [%]	4.82	29.65	65.53	5.10	29.15	65.75
Average surface area [µm²]	7535.89	2887.03	1384.71	7809.93	2914.69	1381.72
Total surface area [mm²]	4.89	11.53	12.22	5.51	11.77	12.58

Table 6. Number of pores, percentage share, total surface area and average values of pore orientation, eccentricity and flattening for groups a, b and c.

Variable	Test 1			Test 2		
	Group A	Group B	Group C	Group A	Group B	Group C
Number of pores [u]	9114.00	2966.00	1387.00	9640.00	3075.00	1132.00
Share [%]	67.68	22.02	10.30	69.62	22.21	8.18
Total pore surface area [mm²]	19.60	6.25	2.79	21.20	6.45	2.21
Average orientation value [°]	12.84	42.51	73.81	13.05	42.04	73.90

 doi:10.20944/preprints202410.1418.v1

Average eccentricity [–]	0.55	0.46	0.39	0.57	0.48	0.40
Average flattening value [–]	0.89	0.84	0.79	0.90	0.85	0.80

In the next stage of the analysis, the individual groups of nonwovens, which had previously been divided in terms of pore surface area (A, B, C) and orientation of the pore angle (a, b, c), were compiled with each other. As a result of the round-robin comparison, 9 detailed subgroups were created, marked successively as Aa, Ab, Ac, Ba, Bb, Bc, Ca, Cb and Cc. The average values obtained for each group with a breakdown in terms of area (large, medium and small ones) and pore angle orientation (vertical, oblique and horizontal ones) for Test 1 and Test 2 are shown in Tables 7 and 8, respectively. Table 9 contains the percentage of the number of areas detected in each group, separated by area size and pore orientation for Test 1 and Test 2, respectively.

Table 7. Number of pores, average pore surface area, and average values of pore orientation, eccentricity and flattening for groups Aa, Ab, Ac, Ba, Bb, Bc, Ca, Cb and Cc received in Test 1.

Variable	Group								
	Aa	Ab	Ac	Ba	Bb	Bc	Ca	Cb	Cc
Number of pores [u]	465.00	140.00	44.00	2722.00	867.00	404.00	5927.00	1959.00	939.00
Average pore surface area [μm²]	7548.40	7494.97	7533.85	2894.31	2876.88	2859.70	1384.78	1381.63	1390.72
Average orientation value [°]	12.07	43.91	73.41	12.65	42.14	74.11	12.98	42.58	73.69
Average eccentricity [–]	0.55	0.43	0.32	0.55	0.45	0.38	0.55	0.46	0.40
Average flattening value [–]	0.89	0.82	0.73	0.90	0.84	0.78	0.89	0.84	0.80

Table 8. Number of pores, average pore surface area, and average values of pore orientation, eccentricity and flattening for groups Aa, Ab, Ac, Ba, Bb, Bc, Ca, Cb and Cc received in Test 2.

Variable	Group								
	Aa	Ab	Ac	Ba	Bb	Bc	Ca	Cb	Cc
Number of pores [u]	521.00	140.00	45.00	2870.00	881.00	286.00	6249.00	2054.00	801.00
Average pore surface area [μm²]	7971.13	7608.18	6571.24	2922.86	2900.38	2876.75	1385.22	1378.10	1363.71
Average orientation value [°]	13.42	41.08	74.40	12.95	41.82	73.71	13.06	42.21	73.93
Average eccentricity [–]	0.56	0.47	0.34	0.57	0.48	0.39	0.57	0.48	0.41
Average flattening value [–]	0.90	0.85	0.75	0.90	0.86	0.79	0.90	0.85	0.81

Table 9. Percentage of the number of detected areas in each group in relation to area size (large, medium and small ones) and pore orientation (vertical, diagonal and horizontal ones).

Classification Criterium	Test No	Share of the Group [%]								
		Aa	Ab	Ac	Ba	Bb	Bc	Ca	Cb	Cc
Area size	1	71.65	21.57	6.78	68.17	21.71	10.12	67.16	22.20	10.64
	2	73.80	19.83	6.37	71.09	21.82	7.08	68.64	22.56	8.80
Pore orientation	1	5.10	4.72	3.17	29.87	29.23	29.13	65.03	66.05	67.70
	2	5.40	4.55	3.98	29.77	28.65	25.27	64.82	66.80	70.76

3.2. Tensile Strength Results

Non-wovens produced with carding machine No. 1 (Test 1) and carding machine No. 2 (Test 2) were subjected to tensile strength tests. The tests were carried out using the Zwick Z050 testing machine in accordance with ISO 9073-3:2023 standard [46]. The samples were stretched in two directions, defined as machine direction (MD) and cross direction (CD), respectively. The strength results obtained were averaged over the width of the production line and are shown in Figures 6.

As can be seen from the strength measurement results shown, the non-woven samples taken from Test 1 (produced on carding machine No. 1) have a higher strength in both directions, i.e., MD and CD, when compared to samples from Test 2, produced on carding machine No. 2. It is related to

 doi:10.20944/preprints202410.1418.v1

the different structural construction of the carders and their effect on fibre mixing and the resulting porosity between the fibres. A detailed analysis of these correlations is presented in Section 4.

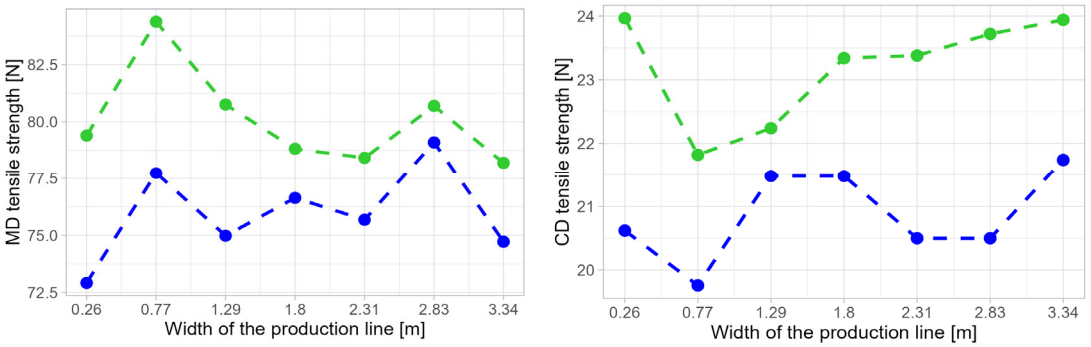

Figure 6. Average tensile strength values in machine direction (**a**) and cross direction (**b**) obtained in the spunlace non-woven tensile tests in Test 1 (green) and Test 2 (blue) relative to the width of the production line.

4. Discussion and Conclusions

The research carried out and described in the paper was aimed at analysing the effect of free spaces, i.e., pores occurring in the spunlace non-woven fabric between bound polyester and viscose fibres on the machine direction (MD) and cross direction (CD) tensile strength of these non-wovens. In addition, the analysis of non-woven images made it possible to compare the carding process on two structurally different carding machines [47].

As part of the research, an analysis of non-woven fabric produced from raw materials characterized in Section 2.1 was carried out in the studies described in Section 3.1 due to the size and distribution of pores, and the strength of this non-woven fabric was experimentally determined, taking into account two different structural construction of carding machines. The number of pores formed is comparable for non-wovens produced with carding machine No. 1 and carding machine No. 2, and their number is 13,467 for carding machine No. 1 and 13,847 for carding machine No. 2, respectively. Differences were observed in pore size, orientation and shape, presented in detail with various aspects in Tables 2÷9.

When comparing the groups resulting from the division, in terms of the pore surface area (Table 5), the number of pores for groups A and B is comparable. In contrast, a significant difference in the number of smallest pores (group C) was noted, there being more of them in Test 2 than in Test 1. In addition, the average area of large areas is definitely larger in Test 2. It affects the strength of the non-woven fabrics tested, which is higher in both machine (MD) and cross directions (CD) for the non-woven fabric produced in carding machine No. 1.

The division in terms of orientation (Table 6) shows that there are more vertical areas in Test 2, while there are significantly more horizontal areas in Test 1. Vertically oriented pores, especially those with a large surface area, affect the result of the cross-stretching test of the CD. In the non-woven fabrics tested, such areas definitely dominate in the non-woven fabric produced by carding machine No. 2, which is visible in its lower CD strength. The number of the largest areas oriented horizontally from the Ac group for carding machines No. 1 and No. 2 is identical.

Within each group resulting from classification in terms of pore surface area, most are vertical in orientation (groups Aa, Ba, Ca), while there are fewer with a diagonal orientation (Ab, Bb, Cb) and least with a horizontal orientation (Ac, Bc, Cc), which is related to the fact that most fibres are arranged according to the direction of production (Tables 7 and 8). Regardless of size, vertically oriented pores are more stretched than horizontal-oriented pores, as indicated by the values of the e and f parameters (Tables 7 and 8). The average size of the large, vertically oriented areas (Aa) is higher for the carding machine No. 2 than for the carding machine No. 1. On the other hand, for areas with

 doi:10.20944/preprints202410.1418.v1

horizontal orientation (Ac), this value is significantly higher for carding machine No. 1. In the case of medium and small areas, their size is comparable regardless of orientation (Tables 7 and 8).

Analysing the percentage of the number of areas detected in each group against the size of the surface area and pore orientation for Tests 1 and 2 (Table 9), it was observed that there were more obliquely oriented and less vertically oriented large areas (A) for Test 1 compared to Test 2. For the medium (B) and small (C) areas, there is apparently more horizontal and less vertical orientation in Test 1 than in Test 2. In the case of horizontal orientation (c) in Test 1, we have more areas of medium and fewer areas of small area size compared to the averaged results obtained in Test 2 (Figure 7).

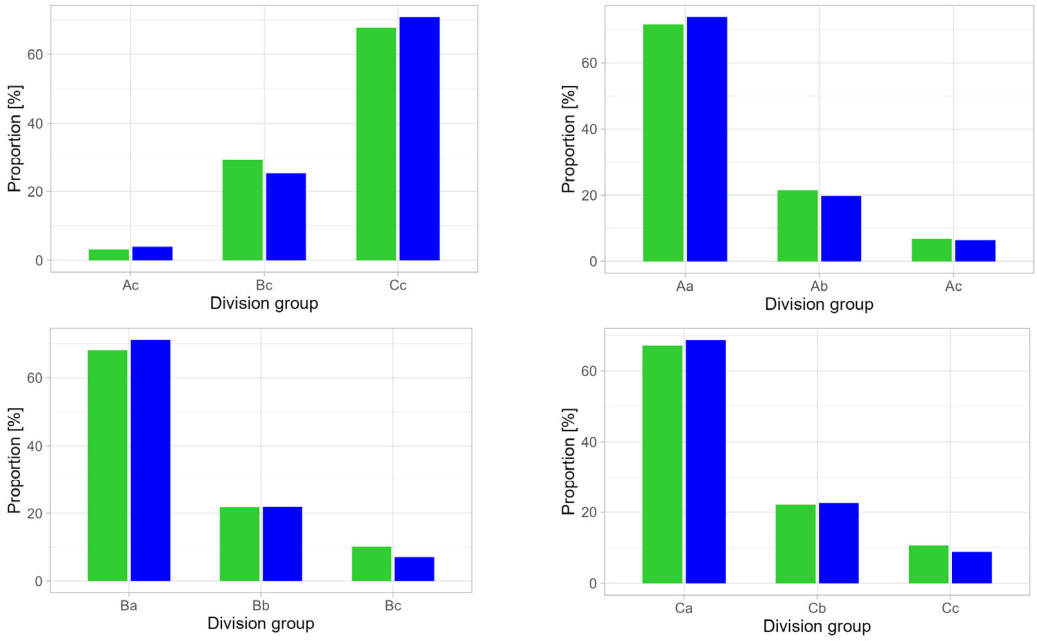

Figure 7. Significant differences in the percentage of the number of areas detected in each group in relation to area size and orientation pores for Test 1 (green) and Test 2 (blue).

The non-woven fabrics tested show different pore characteristics. The distribution of the different pore groups analysed significantly impacts the strength of the non-wovens produced in carding Tests 1 and 2. It was observed that the number, orientation, size and shape of the non-woven fabrics produced with carding machine No. 1 influenced its better machine and cross direction tensile strength compared to the non-woven fabric obtained with carding machine No. 2. The tests carried out allowed carding machine No. 1, to be identified in which a better quality of mixing and a more favourable orientation of the polyester and viscose fibres in the manufacturing process was obtained.

The research carried out showed that the fibres mixing method based on different ways of the carding process is an important element in increasing the strength of non-woven fabric. Based on the tests carried out (Test 1 and Test 2), attention was drawn to the significance of how fibres of different lengths (polyester and viscose) are mixed, thus affecting the strength of the entire non-woven fabric (MD/CD ratio). Using carding machines of different structural construction, the relationship of the fibre mixing method to the strength of the non-woven fabric produced was investigated. It allowed attention to be drawn to a forward-looking trend in the design of modern carders. In view of the textile industry's expectations, which are directed at increasing the efficiency of the process while at the same time increasing the strength of the non-wovens, it is possible to point to features that ensure a more complete fibre bond. Undoubtedly, they include design solutions that provide increased fibre bonding time through repeated blending. The best solution would be to build large-diameter main drum carders with many worker-stripper sub-assemblies. However, this is technically and economically unjustifiable or even impossible. As outlined above, it is important to find mutual dependencies between the method of mixing fibres, the number, size and direction of the resulting

 doi:10.20944/preprints202410.1418.v1

pores and the relationship between the method and the strength of the non-woven fabric. The dependencies are the basis for improving the manufacturing process in order to obtain satisfactory process conditions, ensuring the expected efficiency of non-woven fabric production with the expected strength properties at economically justified costs.

Author Contributions: Conceptualization: A.D.D.-D., W.W. and M.S.(Michał **Szota**); Methodology: M.S.(Michał **Sąsiadek**) and M.N.; Validation: A.D.D.-D., M.S.(Michał **Sąsiadek**) and M.N.; Formal analysis: W.W., M.N. and M.S.(Michał **Szota**); Investigation: M.S.(Michał **Sąsiadek**), W.W. and M.N.; Resources: A.D.D.-D., W.W. and M.S.(Michał **Szota**); Writing—original draft preparation: A.D.D.-D. and M.S.(Michał **Sąsiadek**); Writing—review and editing: M.S.(Michał **Sąsiadek**), W.W. and M.N.; Visualization: M.N.; Supervision: A.D.D.-D. All authors have read and agreed to the published version of the manuscript.

Funding: This research received no external funding.

Institutional Review Board Statement: Not applicable.

Informed Consent Statement: Not applicable.

Data Availability Statement: All the data/references are provided in the manuscript.

Conflicts of Interest: The authors declare no conflict of interests.

References

1. Making the materials to drive Europe's energy revolution, SETIS Magazine 8 (2015) pp. 24-25, SETIS magazine. No. 8 – February **2015,** Materials for energy - Publications Office of the EU (europa.eu), Access: 09.05.2024.
2. Materials 2030 Manifesto, Feb 2022 https://www.ami2030.eu/wp-content/uploads/2022/06/advanced-materials-2030-manifesto-Published-on-7-Feb-**2022.**pdf, Access: 09.05.2024.
3. Tong, L. et al. Re-use of jute fiber hybrid nonwoven breather within laminated composite applications: A case study. *SM&T* **2023**, 36, e00621.
4. Abrishami, S. et al. Textile Recycling and Recovery: An Eco-friendly Perspective on Textile and Garment Industries Challenges. *TEXT RES J* **2024**, 00405175241247806.
5. Hawley, J.M.T. *Textile recycling. Handbook of recycling*; Elsevier, **2014**; pp. 211-217.
6. Advanced Materials **2023** Initiative https://www.ami2030.eu/, Access: 09.05.2024.
7. Materials 2030 Roadmap, Dec **2022** https://www.ami2030.eu/wp-content/uploads/2022/12/2022-12-09_Materials_2030_RoadMap_VF4.pdf, Access: 09.05.2024.
8. Dobrzańska-Danikiewicz, A.D. et al. Characteristics of MWCNTs-Re nanocomposites with a varied Re mass fraction, *NAX* **2017**, 7, 1-8.
9. Dobrzańska-Danikiewicz, A.; Łukowiec D. Synthesis and characterization of Pt/MWCNTs nanocomposites, *PSS* **2015,** 251(12), 2569-2574.
10. Wang Y. New Materials in Textile Innovation. *J. Mater. Process. Des.* **2023**, 7(1), 32-40.
11. Kamiński, K. et al. Hydrogel bacterial cellulose: a path to improved materials for new eco-friendly textiles. *Cellul.* **2020**, 27, 5353-5365.
12. Stanković, S.B. et al. Novel engineering approach to optimization of thermal comfort properties of hemp containing textiles. *J. Text. Inst.* **2019**, 110, 1271–1279.
13. Wei, D.W. et al. Superhydrophobic modification of cellulose and cotton textiles: Methodologies and applications. *J. Bioresour. Bioprod.* **2020**, 5, 1–15.
14. Nayak, R.; Lalit J.; Asimanda K. Traditional fibres for fashion and textiles: Associated problems and future sustainable fibres. In *Sustainable fibres for fashion and textile manufacturing*. Woodhead Publishing, **2023**; pp. 3-25.
15. Zhu, C. et al. Advanced fiber materials for wearable electronics. *Adv. Fiber Mater.* **2023**, 5, 12-35.
16. Edgar, K.J.; Zhang, H. Antibacterial modification of Lyocell fiber: A review. *Carbohydr. Polym.* **2020**, 250, 116932.
17. Thum, M.D. et al. Dynamic Interference Colors in Electrospun Microfibrous Mats. *Adv. Opt. Mater.* **2022**, 10(16), 2200192.
18. Huang, L. et al. Fiber-based energy conversion devices for human-body energy harvesting. *Adv. Mater.* **2020**, 32, 1902034.
19. Liao, M.; Yer, L.; Zhang, Y.; Chen, T.; Peng, H. The recent advance in fiber-shaped energy storage devices. *Adv. Electron. Mater.* **2019**, 5, 1800456.
20. Wang, L. et al. Hollow Spongy Phase Change Composite Fiber with Heat Storage Behavior via Photo-Thermal Transition. *Fibers and Polym.* **2024**, 25, 1805-1814.
21. Floris, I. et al. Fiber optic shape sensors: A comprehensive review. *Opt. Lasers Eng.* **2021**, 139, 106508.

22. Júnior, H.L.O. et al. Smart Fabric Textiles: Recent Advances and Challenges. *Text.* **2022**, 2, 582–605.
23. Chandler, D.L. 3 Questions: The Rapidly Unfolding Future of Smart Fabrics. https://news.mit.edu/2020/smart-fabrics-future-0508, Access: 20.08.2024.
24. ISO 9092:2019 Nonwovens – Vocabulary.
25. CEN EN 29092:1992 Textiles - Nonwovens – Definition.
26. Wilson, A. Development of nonwovens industry. In *Handbook of Nonwovens*, 2nd ed.; Russell, S.J., Ed.; Woodhead Publishing, **2022**; pp. 1–10.
27. Gharei, R; Russell, S.J. Overview of nonwoven product application. In *Handbook of Nonwovens*, 2nd ed.; Russell, S.J., Ed.; Woodhead Publishing, **2022**; pp. 13–47.
28. Niedziela, M.; Sąsiadek, M.; Woźniak, W. Modelling of the carding process for spunlace nonwovens with particular regard to selected mechanical parameters in a double-drum card. Part 1: modelling of the fibre deck forming process. *TJTI* **2019**, 111, 1-11.
29. Niedziela, M.; Sąsiadek, M.; Woźniak, W. Modelling of the carding process for spunlace nonwovens with particular regard to selected mechanical parameters in a double-drum card. Part 2: Modelling of delay times in the longitudinal mixing process. *TJTI* **2019**, 11, 1-10.
30. Niedziela, M.; Sąsiadek, M.; Woźniak, W. Modelling of the selected mechanical properties of the modern double-drum cards for manufacturing of spunlace nonwovens. *TJTI* **2021**, 112, 1655-1665.
31. Karthik, T. et al. *Nonwovens: Process, Structure, Properties and Applications*. WPI Publishing, **2017**.
32. Russell, S. J. (Ed.); *Handbook of nonwovens*, 1st ed.; Woodhead Publishing, **2006**.
33. Albrecht, W.; Fuchs, H.; Kittelmann, W. (Eds). *Nonwoven fabrics: raw materials, manufacture, applications, characteristics, testing processes*. John Wiley & Sons, **2006**.
34. Batra, S.H.; Pourdeyhimi B. *Introduction to nonwovens technology*. DEStech Publications, Inc, **2012**.
35. Santos, A. S.; Ferreira, P. J. T.; Maloney, T. Bio-based materials for nonwovens. *Cellul.* **2021,** 28**,** 8939-8969.
36. Ivars, L.; Ahmad R.; Soulat, D. Effect of the fibre orientation distribution on the mechanical and preforming behaviour of nonwoven preform made of recycled carbon fibres. *Fibers* **2021**, 9.12:82.
37. Roy, R.; Ishtiaque, S. M. Optimal Design of a Filter Media by Tuning the Structure of Needle Punched Nonwoven: Influence of Carding Parameters. *Fibers Polym.* **2020,** 21(9), 2125-2137.
38. Hu, S. et al. Statistical fiber-level geometrical model of thin non-woven structures. In The 7th Technical Textiles-Present and Future" International Symposium, *TTPF* **2021**, pp. 99-104.
39. Hou, J. et al. Convolutional Neural Network for Extracting 3D Point Clouds of Fibrous Web From Multi-Focus Images. *IEEE Access* **2020,** 8, 87857-87869.
40. Chen, Y. et al. Structural characterization and measurement of nonwoven fabrics based on multi-focus image fusion. *Meas.* **2019**, 141, 356-363.
41. Kim, D. Quantitative Evaluation of Geotextile Void Structures Using Digital Image Analysis. *JKES* **2013**, 12(1), 51-61.
42. Stolyarov, O.; Ershov, S. Characterization of change in polypropylene spunbond nonwoven fabric fiber orientation during deformation based on image analysis and Fourier transforms. *J STRAIN ANAL ENG* **2017**, 52(8), 457-466.
43. Otsu N.A. Threshold Selection Method from Gray-Level Histograms. *IEEE T SYST MAN CY-S* **1979**, 9(1), 62-66.
44. Weisstein E.W. Eccentricity, MathWorld, Wolfram Research; https://mathworld.wolfram.com/Eccentricity.html, Access: 20.08.2024.
45. Weisstein E.W. Flattenin, MathWorld, Wolfram Research; https://mathworld.wolfram.com/Flattening.html, Access: 20.08.2024.
46. ISO 9073-3:2023, Nonwovens — Test methods, Part 3: Determination of tensile strength and elongation at break using the strip method.
47. Niedziela, M.; Sąsiadek, M.; Woźniak, W. Pore size, shape and orientation analysis with respect to tensile tests in nonwoven spun-lace textiles using image processing. *TJTI* **2022**, 114(3), 420-432.